Determination of Local Corrosion Current from Individual Harmonic Components

Lukasz Burczyk and Kazimierz Darowicki

Department of Electrochemistry, Corrosion and Materials Engineering, Faculty of Chemistry, Gdansk University of Technology, 80-233 Gdansk, Poland

Harmonic analysis has been used in corrosion measurements for several decades. During this period the method has been refined and developed. Nevertheless, the technique has not been applied to properties determination in local scale yet. This paper is focused on local corrosion current measurements based on harmonic analysis. For this purpose, a non-linear nature of electrode processes is used and measured in local scale applying Harmonic Analysis Microscope (HAM).

DOI: 10.1149/2.1001713jes

The basis of harmonic analysis (HA) is perturbation of the system under investigation with alternating current signal and successive analysis of its feedback in the frequency function. As electrochemical and corrosion processes are non-linear, a polyharmonic signal responds to perturbation. Given the polyharmonic signal, particular harmonic components can be extracted and the values of required kinetic parameters can be calculated thanks to an applicable mathematical approach.

Dévay and Mészáros assumed that the processes of non-faradaic current flow are linear, so they do not generate higher harmonic response than the first component.[1] In respect to non-linear nature of electrode processes, the current signal occurs due to electrode perturbation together with a sinusoidal signal. The current signal consists of a total number of harmonic components displaying the dispersion of frequency.

The main advantage of HA is that corrosion current and both Tafel coefficient can be obtained by single measurement. Subsequently, the measurement of corrosion rate does not employ presumed values for the Tafel slopes. The advantage of this method, comparing to impedance measurements, is the application of a single frequency. In addition, perturbation signal usually has low amplitude (below 30 mV) which helps to maintain steady state condition. However, under certain circumstances, low amplitude could become a disadvantage. Generated and effective voltage perturbation are not equal. It is caused by the ohmic drop due to solution resistance. The difference between both voltages decreases, when solution resistance is low compared with the polarization resistance. Another important aspect of HA is perturbation frequency. The values below 0.1 Hz are applied in most cases. This condition is dictated by the influence of capacitance current related to charging and discharging of the double layer in higher frequencies. Nevertheless, as it was reported earlier, the upper limit of frequency depends on particular properties of investigated system and assumed relative error.[2]

The majority of measurements in the field of corrosion science, with application of HA, has been performed on iron in acidic and neutral environments.[3,4] Among the first applications was the determination of the corrosion rate at the metal/paint interface.[5] As the authors suggest, the use of HA shall allow recognition of the role of binder quality, pigment quantity and quality, and layer thickness of applied coating. Gill et al. examined mild steel in NaCl solution.[6] The results of HA were comparable to those obtained with well-known electrochemical techniques and gravimetric analysis. Mild steel was also examined in various environments[7] for susceptibility to carbon dioxide corrosion. More complex systems were investigated by Vedalakshmi et al.[8] The work concerned rebar embedded in concrete in various environments with different chloride content. Similar approach was also adapted to real-time corrosion monitoring. For two years and half, the monitoring of copper corrosion rate in bentonite block has been examined.[9] There have also been reports on studies of iron in acidic media in presence of corrosion inhibitors.[10]

At the beginning HA was limited to processes where both reactions were activation controlled or one of the reaction was under full-diffusion control. In that case, the harmonic analysis results are not questionable. However, the attempts of HA application to the systems with different controlling factors were made. Bosh et al. examined mild steel in 0.5 M Na_2SO_4, presenting mathematical model which applies to the reaction where anodic process is under activation control, but cathodic reaction is under mixed control.[11] The obtained results were confirmed by Tafel extrapolation. For corrosion current calculation two extra parameters were required: diffusion coefficient and concentration profile of the oxidant. Jankowski also attempted to analyze more complex systems.[12]

Nonetheless, it is worth to notice that all of these results are global harmonic response of total investigated object. Rarely is a sample homogenous, thus conventional electrochemical measurements present response over the entire electrode/electrolyte interface. No information on localized electrochemical reactions is provided in the process of response analysis, which causes data misinterpretation. Investigating the material in local scale, it is possible to detect active and passive sites and measure their impact on material global properties.

The local approach to corrosion measurements was presented in the work of Galica et al.[13] The studies were performed on magnesium alloy to investigate contribution of particular phase into overall corrosion rate. Thanks to Local Electrochemical Impedance Spectroscopy, it was possible to determine differences in corrosion rate of particular phases. Nevertheless, the impedance measurements implement a set of frequencies. Thus, the application of HA to local measurements should decrease time required for parameters mapping due to single frequency perturbation.

This paper is focused on determination of local corrosion current based on harmonic analysis. For this purpose, a non-linear nature of electrode processes is used and measured in local scale applying Harmonic Analysis Microscope (HAM). The advantage of utilized approach base on receiving simultaneous information on corrosion current and both Tafel coefficients, during a single measurement. Therefore, HAM allows determination of local changes of corrosion process kinetics, particularly important when evaluating the role played by microstructure of an alloy.

Experimental

The electrochemical measurements were performed by means of Autolab PGSTAT30 potentiostat/galvanostat (Ecochemie, The Netherlands). The system was expanded with NI PXI-4461 and NI PXI-4462 (National Instruments, USA) measurement cards for AC signal generation and acquisition, respectively. The aforementioned cards were operating in NI PXI-1031 chassis and controlled by NI PXIe-8105 embedded controller.

The measurements were carried out in five-electrode system. The conventional part consists of platinum counter electrode (CE), silver/silver chloride reference electrode (RE) and the investigated metal acting as a working electrode (WE). Two additional electrodes act

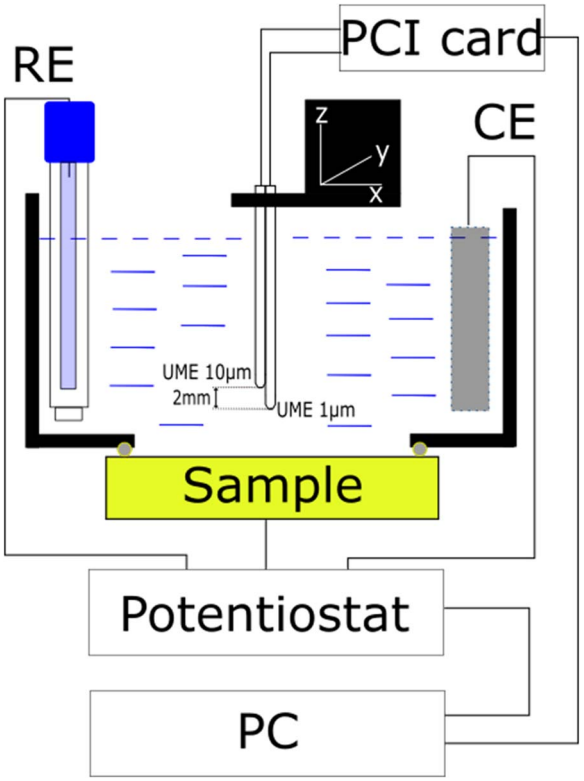

Figure 1. Schematic representation of measuring equipment.

as a twin-electrode. They consist of two ultramicroelectrodes (UME) made of platinum with different diameters: 1 µm and 10 µm, respectively. The smallest electrode was placed 5 µm away from the sample surface, and the second electrode was 2 mm away from the first one in the bulk of solution. The design of the twin-electrode resembles standard probe used in Local Electrochemical Impedance Spectroscopy (LEIS). Due to low spatial resolution of commercial electrodes variations with two UME were applied as a probe.[14,15] During the initial measurements, two setup of different probe diameter were evaluated. Utilization of 1 µm – 1 µm setup resulted in high distortion of detected signal frequencies. This problem has not occurred in a setup with 1 µm – 10 µm microelectrodes, therefore it is suggested that higher-located electrode requires larger active surfaces. Schematic representation of measuring equipment is presented on Fig. 1.

AC signal with frequency of 5 Hz and amplitude 30 mV (p-p) was generated and applied to working electrode. The voltage drop caused by perturbation signal was measured between two UMEs. The UMEs movement in constant height mode was provided by motors system being a part of Scanning Electrochemical Microscope (Sensolytics, Germany) connected to Autolab 128 N. The distance between the probe and the sample was controlled using CCD camera DMK 21AU04 (ImagingSource, Germany). CCD camera had ocular with micrometer scale and was located perpendicularly to Z-axis of motor system. After calibration with a well-defined pattern, the probe was placed 5 µm away from the sample surface. The scanning area was 50 × 50 µm. Every single time, the map was presented as matrix composed of 2500 points with increment between particular pixels equal to 1 µm. The signal generation, acquisition and analysis of data was carried out by authors' original program made in LabVIEW. It was designed in such a way to enable an on-line visualization of measured data.

The polarization curves were made in the range −/+ 250 mV from open circuit potential versus Ag|AgCl. Potential step was set to 1 mv s^{-1}. Tafel parameters were achieved by computer program Nova 1.11 provided by Autolab producer.

The SEM analysis was carried out by means of S-3400N microscope (Hitachi, Japan) with a tungsten source. The microscope is coupled with energy dispersive spectroscopy (EDS) analyzer UltraDry (ThermoFisher Scientific, USA).

The measurements were performed on M58 duplex brass. With regards to EDS measurements, metal consists of 58.9% zinc and 41.1% copper (wt%). Prior to measurements, the investigated sample was grinded with abrasive paper with increasing grit sized up to 2000. After mechanical preparation, brass sample was subjected to etching solution to reveal the structure. The treatment last for 60 second in etching solution composed of 100 cm^3 H_2O, 30 cm^3 HCl and 5 cm^3 $FeCl_3$.[16] The efficiency of etching was determined by Scanning Electron Microscope.

The sample area submitted to electrochemical investigations was 2 cm^2. A solution of 0.1 M KCl was used as an electrolyte. The conductivity of solution was 12.3 mS cm^{-1}. The solution was aerated prior to each experiment. During the experiment, the sample was held at open circle potential ($E_{OCP} = -0.19$ V vs Ag|AgCl).

Results and Discussion

For the purpose of this work, the local corrosion rate was calculated on the basis of particular harmonic component. The measured drop of the voltage caused by perturbation signal between UME was subjected to Short-Time Fourier Transformation. The obtained spectrum was analyzed in order to describe values of the fundamental, the second and the third harmonic component. The amplitudes of particular harmonic were determined from the spectrum automatically by the authors' original program. The amplitudes of harmonic potential were calculated to local current according to Equation 1 with respect to Ohm's law:[17]

$$i(\omega)_{loc} = \frac{\Delta V(\omega)_{probe}\kappa}{d} \qquad [1]$$

where $i(\omega)_{loc}$ is a value of local current, $\Delta V(\omega)_{probe}$ is a drop of voltage measured between UME, κ is conductivity of the solution and d is distance between UMEs. As a result, the set of parameters was obtained, including fundamental, second and third harmonic current values with specific coordinates.

As the anodic and cathodic charge transfer reaction is non-linear, the form of faradaic current is a distorted sinusoid.[1] Consequently, the faradaic current consists of fundamental harmonic component with frequency of ω and higher harmonics with frequencies of kω (k = 2, 3...). Using the Fourier series, it is possible to describe faradaic current as follows:

$$\begin{aligned} i_F = i_{corr}\Bigg\{\Bigg[I_0\left(\frac{U_0}{\beta_a}\right) + 2\sum_{k=0}^{\infty}(-1)^k I_{2k+1}\left(\frac{U_0}{\beta_a}\right) sin\,(2k+1)\,\omega t \\ + 2\sum_{k=1}^{\infty}(-1)^k I_{2k}\left(\frac{U_0}{\beta_a}\right) cos 2k\omega t\Bigg] e^{\frac{\Delta E}{\beta_a}} \\ -\Bigg[I_0\left(\frac{U_0}{\beta_c}\right) - 2\sum_{k=0}^{\infty}(-1)^k I_{2k+1}\left(\frac{U_0}{\beta_c}\right) sin\,(2k+1)\,\omega t \\ + 2\sum_{k=1}^{\infty}(-1)^k I_{2k}\left(\frac{U_0}{\beta_c}\right) cos 2k\omega t\Bigg] e^{-\frac{\Delta E}{\beta_c}} \end{aligned} \qquad [2]$$

where I_n (n = 0, 1, 2...) are modified Bessel functions of the first kind.

The equation presented above allows to determine the value of current for each of the first three harmonic components. For the purpose of mathematical model simplification, the assumption that amplitude U_0 is limited to the extent that the Bessel function could be approximated with Taylor polynomials is applied. In such case, the equations describing particular harmonic components could be presented as

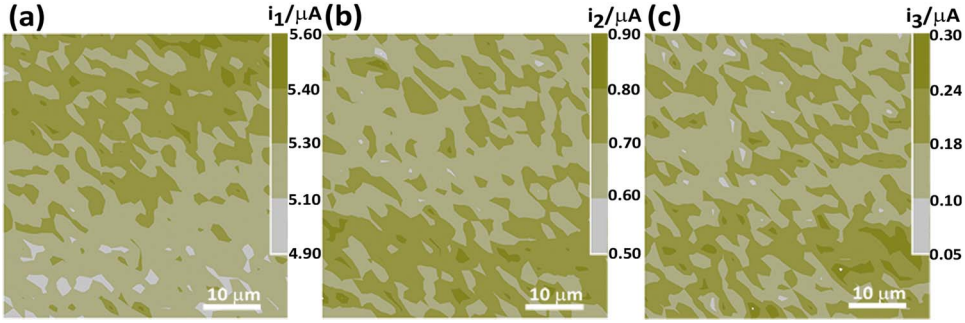

Figure 2. Current maps of particular harmonic component, (a) fundamental harmonic, (b) second harmonic, (c) third harmonic.

follows:

$$i_1 = i_{corr} U_0 \left[\left(\frac{1}{\beta_a} \right) + \left(\frac{1}{\beta_c} \right) \right] \quad [3]$$

$$i_2 = i_{corr} \frac{U_0^2}{4} \left[\left(\frac{1}{\beta_a^2} \right) - \left(\frac{1}{\beta_c^2} \right) \right] \quad [4]$$

$$i_3 = i_{corr} \frac{U_0^3}{24} \left[\left(\frac{1}{\beta_a^3} \right) + \left(\frac{1}{\beta_c^3} \right) \right] \quad [5]$$

where i_n is harmonic current, i_{corr} corrosion current, U_0 applied amplitude of perturbation, β_a and β_c are Tafel coefficients for anodic and cathodic reaction, respectively.

Selecting appropriate frequency is crucial due to influence elimination of capacitance current. Low frequency (below 0.1 Hz) is usually applied in case of harmonic analysis. However, the lower the frequency, the longer the acquisition time. In scanning mode of such low frequency, the time required to obtain at least three waveforms for harmonic analysis at a single measuring point would be a great disadvantage. During this time, the condition of the investigated system could change and two consecutive points would be described by different conditions. The frequency was selected according to Sathiyanarayanan[2] work based on the knowledge about polarization resistance R_p and double layer capacitance C_{dl}. For the measurements to be reliable, R_p should be greater than $(\omega C_{dl})^{-1}$. This condition is fulfilled, when the frequency is lower than 5.5 Hz. On the other hand, equation proposed by Jankowski[12] was used to verify the level of relative error during fundamental harmonic current measurement. Therefore, we can calculate that this error is less than 0.1%. Summarizing, the upper limit of frequency depends on properties of particular system and assumed relative error. Thus, the frequency should be selected individually for specific investigated system.

The magnitude of amplitude of individual harmonic components depends on properties of the investigated system and resistance of the environment.[18] For this reason, a perturbation amplitude has to be chosen with respect to achieve steady-state conditions and sufficient response of each component. In the case of corrosion current determination, the fundamental, the second and the third harmonics are of main interest. Harmonic of higher number could be neglected. Each higher harmonic signal has lower response than the former one. Thus, the assumption about value of the highest signal number is needed. The amplitude of perturbation signal was chosen with the assumption that amplitude of third harmonic signal should attain 0.1% of that of the entire signal. In particular, the third harmonic might be undetectable if the perturbation amplitude, electrolyte conductivity or measurement card resolution are too low. If such situation appears, the third harmonic might be mistaken with the background noise, producing substantial measurement errors. The applied self-made data acquisition program, written in LabView environment, allows to monitor whether amplitude of the third harmonic is measurable and higher than background noise. Similar approach is used during dynamic impedance measurements.[19,20]

The obtained maps of the particular harmonic are presented on Fig. 2. Each successive signal is characterized by a lower magnitude, in accordance with the theory. Furthermore, the high level of correlation can be distinguished between the second and the third harmonic map, as expected. Simultaneously, fundamental harmonic response is quite the opposite.

Equations 6–8 describe relationship between individual harmonic components from specific parameters of system. Corrosion current may be calculated on the basis of the first three harmonic components separated from the signal, which require solving Eqs. 3–5.

$$i_{corr} = \frac{i_1^2}{4\sqrt{3}\ \ 2i_1|i_3| - i_2^2} \quad [6]$$

If $\beta_c > \beta_a$

$$\frac{1}{\beta_a} = \frac{1}{2U_o} \left(\frac{i_1}{i_{corr}} + 4\frac{|i_2|}{i_1} \right) \quad [7]$$

$$\frac{1}{\beta_c} = \frac{1}{2U_o} \left(\frac{i_1}{i_{corr}} - 4\frac{|i_2|}{i_1} \right) \quad [8]$$

It was possible to calculate local corrosion rate by implementing equation 6 with respect to data presented on Fig. 2. Diard et al.[21] discussed modification of Eq. 6 taking into account correlation between first and third harmonic. However, it is justified to neglect this modification for as long as Fourier transformation is used to extract particular component of harmonics and all components are measured simultaneously. Furthermore, the third harmonic component gives contribution of approx. 0.1% of the entire signal. The assumption made in Equations 3–5 causes error of about 10%, so neglecting the contribution of third harmonic in the first one is acceptable and does not generate higher error in the final result.

It should be noted that the above mathematical formulas and the approach overall is restricted to processes where both anodic and cathodic process are activation controlled.[1,12,22,23] For full diffusion control of one of the processes ($\beta_{a,c} \to \infty$) or under mixed control, mathematical description is different.[12]

The local current map, calculated with Equation 6 is presented on Fig. 3b. Two main areas can be distinguished, characterized by differences in corrosion current values. Created local current path should be associated with brass structure presented on Fig. 3a. Phases size and distribution can be observed. The structure of investigated duplex brass consists of two phases: α- and β-phase,[24–26] the primary difference is zinc contribution. In β-phase contribution of zinc is higher than α-phase. If the brass is exposed to corrosive environment, different structure leads to formation of galvanic microcells, where β-phase acts as an anode and α-phase as a cathode.

It is important to state that both presented images do not represent the same region of sample surface. However, similar pattern could be distinguished between both figures. Higher corrosion current represents areas of β-phase, while lower values should be associated with α-phase.

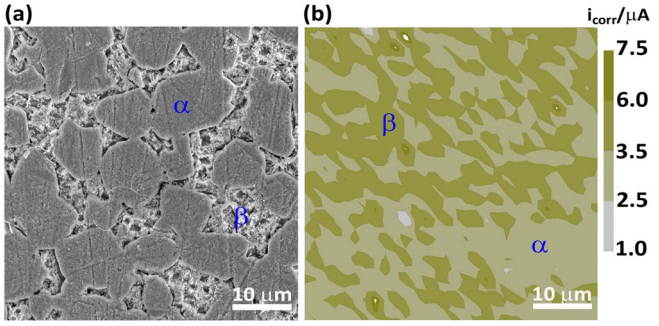

Figure 3. Scanning electron image of brass surface prior to measurements (a). Map of calculated local current over brass (b).

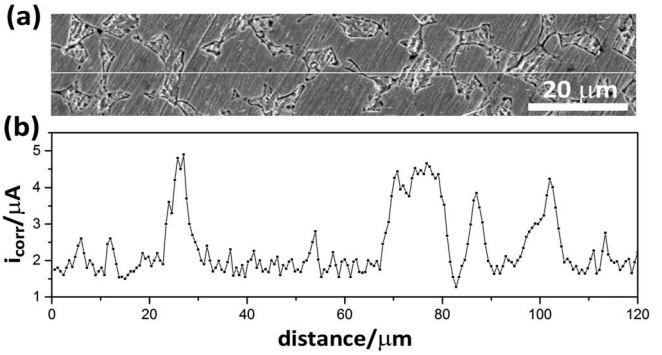

Figure 5. SEM image of the sample surface with a white line corresponding to place of measurement (a), and graph representing changes of corrosion current based on HA across the white line (b).

According to Equations 7–8, calculation of both β coefficients is possible based on HA measurements. The spatial distribution of particular parameters is presented on Figs. 4a and 4b. Both coefficients are higher in areas where corrosion current increases according to Fig. 3b. Nonetheless, it is worth to notice that β_c is locally characterized by high values. Such behavior would imply that the dynamics of the cathodic reaction (oxygen depolarization, in neutral pH) is locally diversified. There are few possible reasons for such behavior, such as difference in local oxygen demand or locally altered adsorption of oxygen to the active sites. Moreover, the changes in β_c Tafel slope lead to different corrosion currents. When the slope is rising, the current increases as well.

It should be noted that according to Equations 7–8 calculated Tafel coefficients depend on perturbation amplitude U_0, as was also discussed by Gabrielli et al.[27] It was concluded that high correlation between obtained results was visible for perturbation amplitudes no greater than 30 mV. Higher values of U_0 should not be considered due to limitation resulting from application of Besell function.[1,27]

In order to determine the type of control, series of Tafel plot were made. Polarization curves, as shown in Fig. 4c, are characterized by activation control of cathodic and anodic process. Average values of i_{corr} and both β coefficients resulting from Tafel's plot with their standard deviation have been presented on Fig. 4d. Furthermore, the average values of the same parameters based on harmonic measurements were added for comparison. The results of both experiments are correspondent.

In order to compare changes of corrosion current with material structure, an additional measurement was made. The main objective of the measurement was one to one correlation of SEM image and corrosion current changes. For the purpose of measurement, sample surface was significantly limited through coverage by insulator. Series of line scans were performed in the limited area. Subsequently, the relevant areas were photographed with SEM in order to compare the results. The obtained corrosion current dependency from the distance was presented on Fig. 5b. Presumably, the corrosion current increased when the probe was located above β-phase, while decreasing over α-phase. For comparison, Fig. 5a presents a white line to mark the place

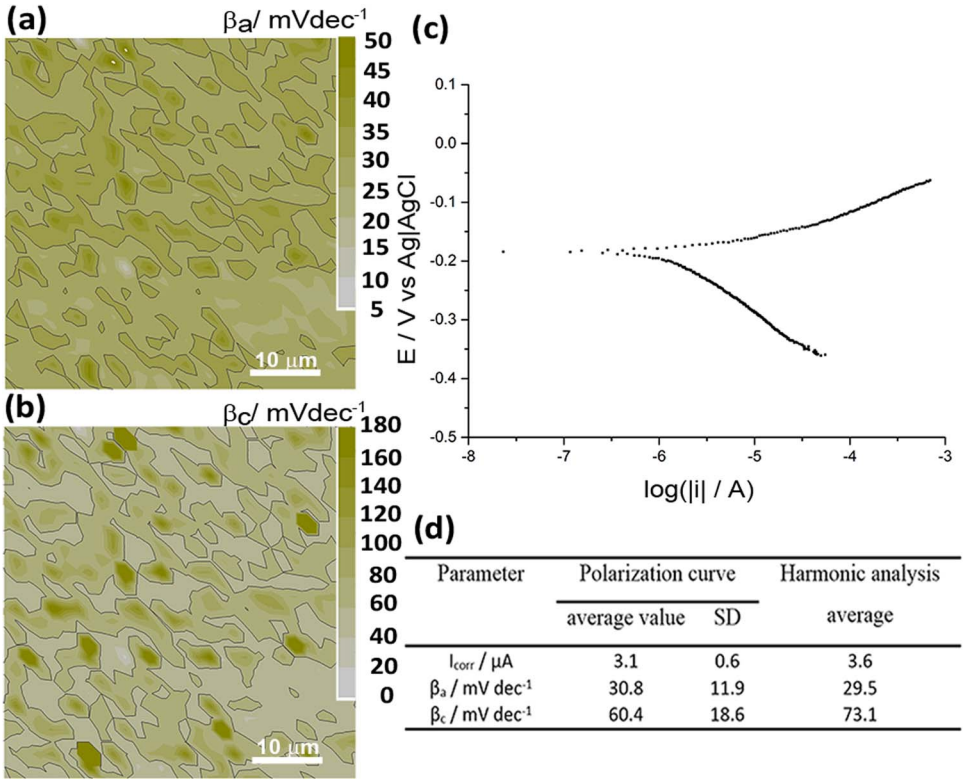

(d)

Parameter	Polarization curve		Harmonic analysis
	average value	SD	average
I_{corr} / μA	3.1	0.6	3.6
β_a / mV dec^{-1}	30.8	11.9	29.5
β_c / mV dec^{-1}	60.4	18.6	73.1

Figure 4. Beta coefficients (a) for anodic reaction, (b) for cathodic reaction. Tafel plot (c) and (d) comparison of data obtained by polarization curves with standard deviation against average from harmonic one.

of measurement. What is worth to mention is that with respect to diffusion field, the line scan may have been performed a few micrometers below or above the marked line.

Conclusions

The application of harmonic response in local scale was presented. Using appropriate measuring setup and mathematical approach, it is possible to calculate corrosion current and both Tafel coefficients in microscale. In case of harmonic response analysis in scanning mode choice of appropriate frequency is crucial for reasonable time of experiment, and therefore, reliable results.

It is crucial to emphasize that presented values with HAM technique were obtained by equation which consists of certain approximation described in this work. Nevertheless, applying of harmonic analysis in local scale allowed to reveal differences in corrosion current of particular phases.

Acknowledgment

The authors gratefully acknowledge the financial support from the Polish National Science Centre (NCN) under grant no. 2015/19/N/ST5/02659. The authors thank prof. Artur Zielinski for fruitful discussion and help with solving technical problems.

References

1. J. Dévay and L. Mészáros, *Acta Chim. Acad. Sci. Hung.*, **100**, 183 (1979).
2. S. Sathiyanarayanan and K. Balakrishnan, *Br. Corros. J.*, **29**, 152 (1994).
3. U. M. Angst and B. Elsener, *Corros. Sci.*, **89**, 307 (2014).
4. J. J. Kim and Y. M. Young, *Int. J. Electrochem. Sci.*, **9**, 6949 (2014).
5. L. Mészáros, B. Lengyel, and F. Janászik, *Mater. Chem.*, **7**, 165 (1982).
6. J. S. Gill, L. M. Callow, and J. D. Scantlebury, *Corrosion*, **39**, 61 (1983).
7. W. Durnie, R. De Marco, A. Jefferson, and B. Kinsella, *Corros. Sci.*, **44**, 1213 (2002).
8. R. Vedalakshmi, S. Manoharan, H.-W. Song, and N. Palaniswamy, *Corros. Sci.*, **51**, 2777 (2009).
9. B. Rosborg, D. Eden, O. Karnland, J. Pan, and L. Werme, *MRS Proc.*, **807**, 489 (2003).
10. A. Pirnát, L. Mészáros, and B. Lengyel, *Corros. Sci.*, **37**, 963 (1995).
11. R. W. Bosch, *J. Electrochem. Soc.*, **143**, 4033 (1996).
12. J. Jankowski, *J. Electrochem. Soc.*, **150**, B181 (2003).
13. G. Galicia, N. Pébère, B. Tribollet, and V. Vivier, *Corros. Sci.*, **51**, 1789 (2009).
14. J.-B. Jorcin, H. Krawiec, N. Pébère, and V. Vignal, *Electrochimica Acta*, **54**, 5775 (2009).
15. G. Baril, C. Blanc, M. Keddam, and N. Pébère, *J. Electrochem. Soc.*, **150**, B488 (2003).
16. P. Walker and W. H. Tarn, Eds., *CRC handbook of metal etchants*, p. 196, CRC Press, Boca Raton, (1991).
17. R. S. Lillard, P. J. Moran, and H. S. Isaacs, *J. Electrochem. Soc.*, **139**, 1007 (1992).
18. K. Darowicki, *J. Electroanal. Chem.*, **394**, 81 (1995).
19. J. Ryl, L. Burczyk, R. Bogdanowicz, M. Sobaszek, and K. Darowicki, *Carbon*, **96**, 1093 (2016).
20. J. Wysocka, S. Krakowiak, J. Ryl, and K. Darowicki, *J. Electroanal. Chem.*,**778**, 126 (2016).
21. J.-P. Diard, B. Le Gorrec, and C. Montella, *J. Electrochem. Soc.*, **142**, 3612 (1995).
22. L. Mészáros, *J. Electrochem. Soc.*, **141**, 2068 (1994).
23. K. Darowicki and J. Majewska, *Corros. Rev.*, **17** 383 (1999).
24. E. Farabi, A. Zarei-Hanzaki, M. H. Pishbin, and M. Moallemi, *Mater. Sci. Eng. A*, **641**, 360 (2015).
25. J. Ryl, J. Wysocka, P. Slepski, and K. Darowicki, *Electrochimica Acta*, **203**, 388 (2016).
26. C. T. Kwok, H. C. Man, and F. T. Cheng, *Mater. Sci. Eng. A*, **242**, 108 (1998).
27. C. Gabrielli, M. Keddam, and H. Takenouti, *Mater. Sci. Forum*, **8**, 417 (1986).